Denoising Gravitational Wave Signals with Wavelet Packets

Syed Abidi

April 2025

1 Introduction

Gravitational waves are distortions in spacetime first predicted by Albert Einstein and directly observed for the first time in 2015 by the LIGO and Virgo collaborations (see Figure 2). This landmark detection, designated GW150914 (Figure 1), resulted from the inspiral and merger of two stellar-mass black holes. Gravitational wave signals are inherently extremely weak and are often obscured by complex, non-stationary noise. Such noise arises from a variety of sources, including seismic vibrations, thermal fluctuations, and quantum sensing noise.

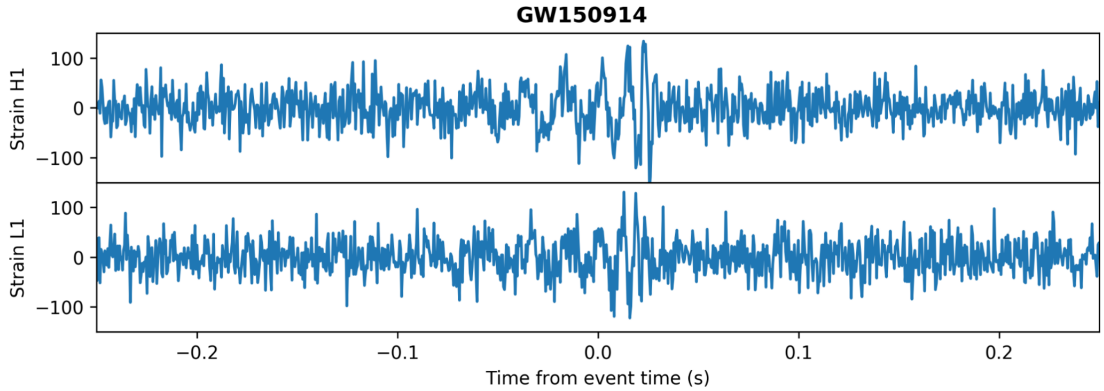

Figure 1: First CBC observation from gravitational waves. [4]

Gravitational waves propagate at the speed of light and carry rich information about the astrophysical systems that generate them, offering a unique observational window into the dynamics of the universe. Among the most significant sources of gravitational waves are compact binary coalescence (CBC) events, involving pairs

of neutron stars or black holes. These systems lose energy through the emission of gravitational radiation, causing the two compact objects to spiral inward over time. The inspiral phase is characterized by a gradual increase in both the amplitude and frequency of the emitted gravitational wave signal, culminating in the merger of the two objects, followed by the ringdown of the newly formed remnant (Figure 3). This evolution can be observed in the characteristic gravitational wave "chirp," where the frequency and amplitude of the signal increase rapidly over a short timescale.

Figure 2: Two LIGO observatories. Courtesy of Caltech/MIT/LIGO Laboratory. [7]

Binary black hole inspirals, a particularly important class of CBC events, are of special interest due to their relatively strong gravitational wave emissions, which allow their detection over cosmological distances. The high sensitivity of the LIGO and Virgo detectors to these events enables detailed studies of the properties of black holes and enhances our understanding of their population and dynamics.

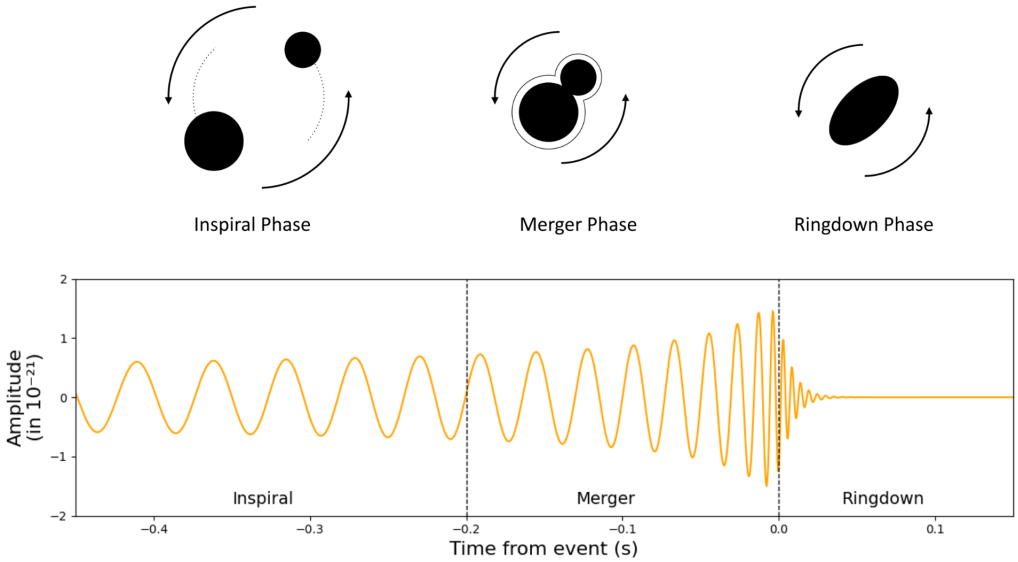

Figure 3: The process of Compact Binary Coalescence that produces the gravitational waves through the 3 stages.

The detection of well-modeled signals, such as binary black hole inspirals, typi-

cally relies on matched filtering, a technique that cross-correlates observational data with a bank of predicted waveform templates to maximize the signal-to-noise ratio (SNR). However, matched filtering presupposes detailed prior knowledge of the signal morphology and can be less effective for unmodeled or unexpected signals. To address these limitations, this work employs traditional signal processing techniques that extract gravitational wave signals from noise without depending on machine learning models or exhaustive template banks. Specifically, we explore a classical approach based on filtering and time-frequency analysis to isolate gravitational wave signals. The proposed methodology combines band-pass filtering, which restricts the signal to the expected frequency range (20–400 Hz), with wavelet-based denoising techniques that operate in the time-frequency domain.

2 Mathematical Background

2.1 Band-Pass Filtering

Band-pass filtering restricts the analysis to a frequency range relevant to gravitational wave signals originating from compact binary coalescence events, particularly binary black hole inspirals. At lower frequencies—typically below 20 Hz—detector sensitivity is heavily affected by seismic and environmental noise, which can obscure the gravitational wave signal. Eliminating these frequencies significantly reduces low-frequency noise contributions without compromising signal integrity, as gravitational waves from CBC events predominantly lie above this range.

Conversely, at higher frequencies—generally above 400 Hz—the amplitude of gravitational wave signals from typical binary black hole inspirals decreases sharply, becoming negligible in comparison to quantum shot noise, which dominates the detector's noise spectrum in that regime. This behavior is illustrated in Figure 4.

Accordingly, our analysis focuses on the frequency band from approximately 20 to 400 Hz, where gravitational wave signals are most pronounced and detector sensitivity is optimal.

In this paper, we implement a Butterworth filter, a type of band-pass filter characterized by its maximally flat amplitude response within the passband and smooth, ripple-free transition to the stopband. The design of the Butterworth filter requires specification of the desired frequency band in normalized units relative to the Nyquist frequency. Given that the gravitational wave data are sampled at 2048 Hz, the corre-

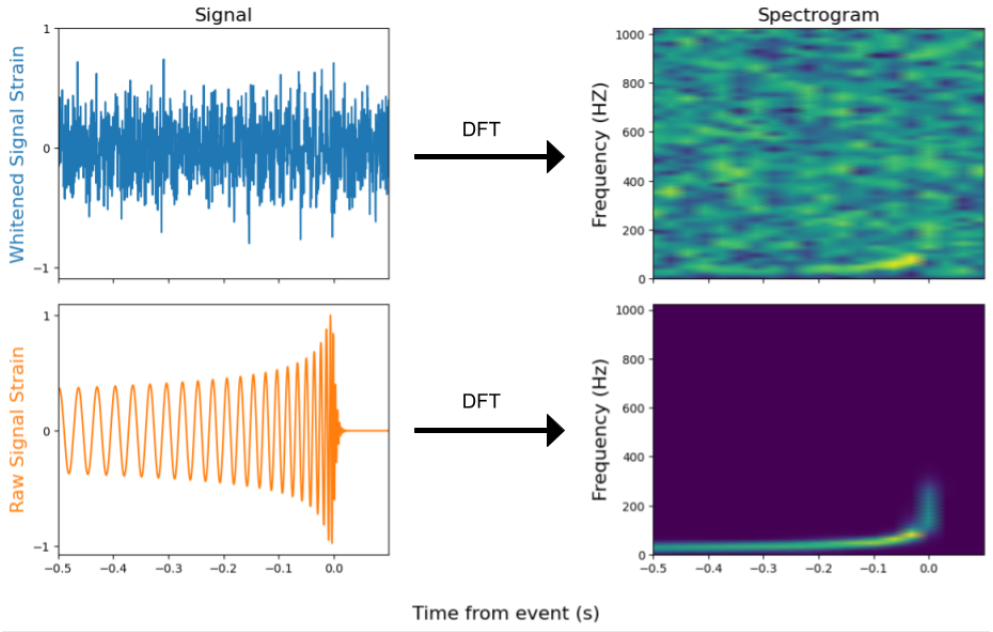

Figure 4: Spectrograms of whitened gravitational wave and raw signal.

sponding Nyquist frequency is 1024 Hz. With a target frequency band of 20–400 Hz, the normalized cutoff frequencies are therefore determined by dividing each cutoff by the Nyquist frequency, yielding normalized values of

$$\text{low cutoff (normalized)} = \frac{20\,\text{Hz}}{1024\,\text{Hz}} \approx 0.0195$$

$$\text{high cutoff (normalized)} = \frac{400\,\text{Hz}}{1024\,\text{Hz}} \approx 0.3906.$$

Filtering in the time domain can be described using the convolution integral between the input signal $x(t)$ and the filter's impulse response $h(t)$:

$$y(t) = (x * h)(t) = \int_{-\infty}^{\infty} x(\tau)h(t-\tau)d\tau \tag{1}$$

In practice, the convolution and data analysis was done discretely where the filtered output $y[n]$ is the discrete convolution with the sampled data $x[n]$. The filtering is done entirely by convolving with a discrete impulse response $h[n]$ of a 5th-order Butterworth band-pass which is derived from the following process:

$$y[n] = \sum_{k=0}^{5} b_k\, x[n-k] \;-\; \sum_{k=1}^{5} a_k\, y[n-k]$$

where $\{b_0, \ldots, b_5\}$ and $\{a_0, \ldots, a_5\}$ are the filter coefficients (computed via bilinear transform for 20–400 Hz). By definition, the impulse response function is given when the unit impulse function $\delta[t]$ is passed in for $x[n]$. As such we get

$$\begin{aligned} h[0] &= \frac{b_0}{a_0}, \\ h[1] &= \frac{b_1 - a_1\, h[0]}{a_0}, \\ &\vdots \\ h[5] &= \frac{b_5 - \sum_{k=1}^{5} a_k\, h[5-k]}{a_0}. \end{aligned}$$

As the final step, the convolution is done discretely to produce the output signal:

$$y[n] = \sum_{k=0}^{M} h[k]\, x[n-k].$$

The digital implementation of this filter uses zero-phase filtering, where the filtering operation is applied forward and backward through the data, ensuring that the output signal $y(t)$ has zero phase distortion relative to $x(t)$.

2.2 Daubechies Wavelet Packet Transform

Following the application of a general band-pass filter, a more refined method is necessary to isolate the sharp variations, or "chirps", characteristic of compact binary coalescence (CBC) events in gravitational wave signals. The residual noise after band-pass filtering still overlaps with the frequency range of the target signals, rendering purely frequency-selective filters insufficient for accurate signal isolation. Moreover, it is crucial to achieve high-frequency resolution along with strong time-frequency localization to effectively capture these transient features. To address these challenges, we employ a wavelet packet transform, utilizing Daubechies wavelets with four vanishing moments and soft thresholding. This approach enables the extraction of fine-scale structures within the signal while preserving its temporal and spectral characteristics to denoise thereafter.

Daubechies wavelets form a family of compactly supported, orthonormal wavelets characterized by having a maximal number of vanishing moments for a given support width. The compact support property ensures that the wavelet function $\phi(x)$ is

nonzero only over a finite interval, specifically

$$\text{supp } \psi = [0, 2n-1],$$

where n denotes the number of vanishing moments. Consequently, the wavelet basis functions are highly localized in time, meaning that sudden changes in the data, such as discontinuities or rapid oscillations, influence only a small, localized set of wavelet coefficients.

Moreover, Daubechies wavelets satisfy the vanishing moment condition:

$$\int_{-\infty}^{\infty} t^k \phi(t)\, dt = 0 \quad \text{for } k = 1, 2, \ldots, n-1$$

where $\phi(t)$ denotes the scaling function. This property implies that Daubechies wavelets are orthogonal to polynomials of degree up to $n-1$. In practical terms, the wavelet transform produces coefficients close to zero for any locally smooth (polynomial-like) portion of the signal, while producing significant coefficients only near regions where the signal exhibits non-polynomial behavior—such as edges, cusps, or "chirp"-like features.

This makes Daubechies wavelets particularly well-suited for detecting and isolating singularities or sharp transitions, which are characteristic of gravitational wave signals from compact binary coalescence events. The chirp signals associated with these events involve rapidly varying frequencies and amplitudes that manifest as localized singularities in the time-frequency domain. By using a wavelet basis that is inherently sensitive to such localized irregularities, while remaining insensitive to smooth background trends, the Daubechies wavelets provide an efficient and effective framework for denoising and feature extraction in gravitational wave data analysis.

Practically, decomposing our signal to find the Daubechie wavelet decomposition coefficients involves convolving the signal with the low-pass filter h and high-pass filter g corresponding the scaling function ϕ and wavelet ψ respectively. Calculating h involves solving a system of nonlinear equation that correspond to targeted number of vanishing moments N. One function is the scaling function equation:

$$\phi(t) = \sum_n h[n]\sqrt{2}\phi(2t-n)$$

where we solve for $h[1], h[2], \ldots h[2N-1]$ receiving $2N$ coefficients. The other equa-

tions include the normalization condition:

$$\int \phi(t)\ dt = 1$$

and the vanishing moments condition described earlier. Once h is computed, g may be derived from:

$$g[n] = (-1)^n h[2N - 1 - n].$$

For this project, we used the `PyWavelet` Python library [5], which provides precomputed values for h and g for standard Daubechies wavelets with four vanishing moments.

The traditional Discrete Wavelet Transform (DWT) applies h and g to the original signal to compute the scalar and wavelet coefficients respectively. Crucially, only the scalar coefficients are used as input for the level of decomposition. This hierarchical scheme is visualized in Figure 5 and is well-suited for signals where the most important features are concentrated at low-frequency bands. However, for gravitational wave signals, particularly those from CBC events, this traditional approach presents limitations. The chirp-like structure of such signals involves localized bursts of information across a broader frequency range. Because the DWT ignores the high-frequency outputs at each level during subsequent decomposition, it risks discarding important signal characteristics that are critical for accurate denoising.

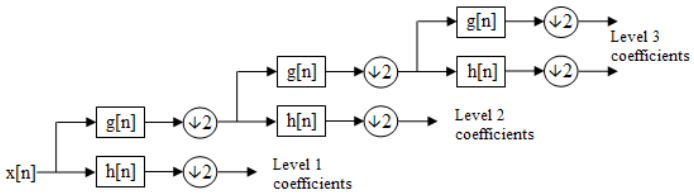

Figure 5: Wavelet Decomposition Diagram. [9]

To address this, we employ the Wavelet Packet Transform (WPT), which generalizes the traditional approach by recursively decomposing both scalar and wavelet coefficients at each level (Figure 6). This full decomposition is particularly advantageous in our use case, where the gravitational wave

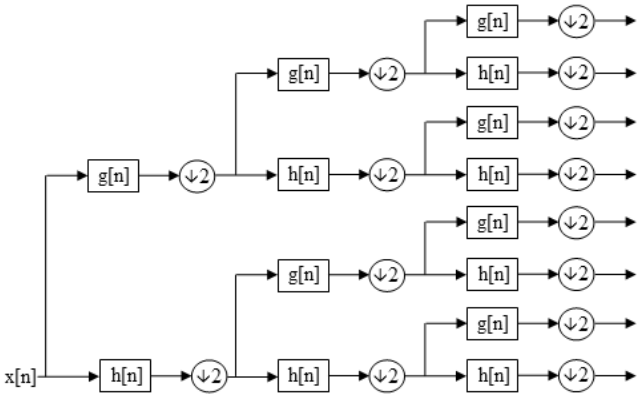

Figure 6: Wavelet Packet Decomposition Diagram. [8]

signal is often buried in broadband noise. By exposing a richer set of frequency components, the WPT enables more precise thresholding strategies to suppress noise while preserving the sharp, localized features of the signal. The choice of decomposition depth (maximum level) plays a critical role in balancing noise reduction and signal preservation, and its optimal value will be explored empirically in Section 3.

2.3 Soft Thresholding

After performing the wavelet packet transform (WPT) decomposition, the finer details of the signal are isolated and prepared for denoising. Soft thresholding was selected as the denoising method due to its effectiveness in preserving signal features while suppressing noise. Gravitational wave signals tend to produce large wavelet coefficients concentrated around singularities, making thresholding an effective approach for isolating these key features. In contrast, the noise is typically distributed across many small-magnitude coefficients. By setting small coefficients to zero while gently reducing the magnitude of larger ones, soft thresholding removes noise without introducing sharp discontinuities in the remaining signal. Mathematically, for each coefficient x, soft thresholding is defined by:

$$T_{\text{soft}}(x, \lambda) = \begin{cases} \text{sign}(x) \cdot (|x| - \lambda), & \text{if } |x| > \lambda \\ 0, & \text{if } |x| \leq \lambda \end{cases}$$

where λ is the threshold value and sign is the sign function that returns the sign of x. The optimal value for λ is determined empirically in Section 3.

2.4 Reconstruction

Following the thresholding step, the denoised signal is reconstructed from the retained wavelet coefficients using the reconstruction lowpass filter $\tilde{h}$ and reconstruction highpass filter $\tilde{g}$ filters. This synthesis process reassembles the denoised signal in the time domain. Ideally, it preserves significant signal features, such as the merger in the CBC event, while minimizing noise suppressed during the thresholding stage.

3 Application & Results

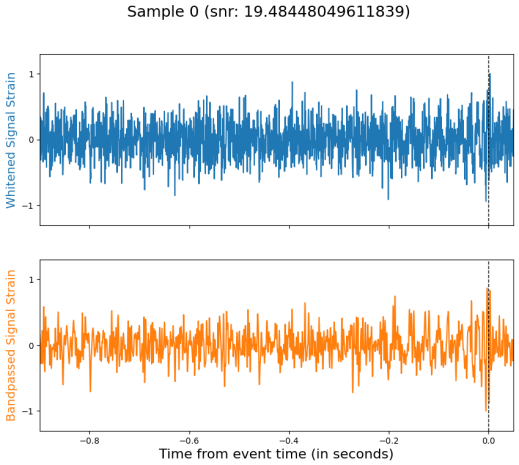

Figure 7: Result from applying bandpass filter to whitened signal.

To generate the data used in this analysis, the `LALSuite` Python package [6] was employed to simulate mathematically accurate gravitational waveforms, which were then injected into synthetic white noise. This approach enables direct comparison against idealized raw waveforms during the denoising evaluation. In particular, the `ggwd` scripts developed by Timothy Gebhard et al. [3] were utilized to produce a dataset consisting of 325 samples of whitened gravitational waves containing compact binary coalescence (CBC) events. Each sample has a duration of 16 seconds, a sampling rate of 2048 Hz, and a signal-to-noise ratio (SNR) between 15 and 20, where the SNR is defined as

$$\text{SNR} = \frac{\text{amplitude of signal}}{\text{standard deviation of noise}}.$$

After applying the bandpass filter described previously (20 Hz to 400 Hz), a substantial portion of extraneous frequencies were removed from the whitened waveform, as shown in Figure 7.

To quantitatively assess the effectiveness of the filtering process, the denoised signal was compared to the original raw waveform using the mean squared error (MSE), defined as

$$\text{MSE} = \frac{1}{n}\sum_{i=1}^{n}(Y_i - \hat{Y}_i)^2$$

where Y denotes the raw signal and $\hat{Y}$ denotes the denoised signal.

The wavelet packet thresholding method introduces two tunable parameters: the maximum decomposition level of the wavelet packet transform and the threshold value λ applied during soft thresholding. To determine the optimal values for these parameters, a grid search was conducted, systematically varying each parameter and recording the resulting mean squared error. Figure 8 presents the results, plotting the selected threshold values against the corresponding mean squared errors for each level.

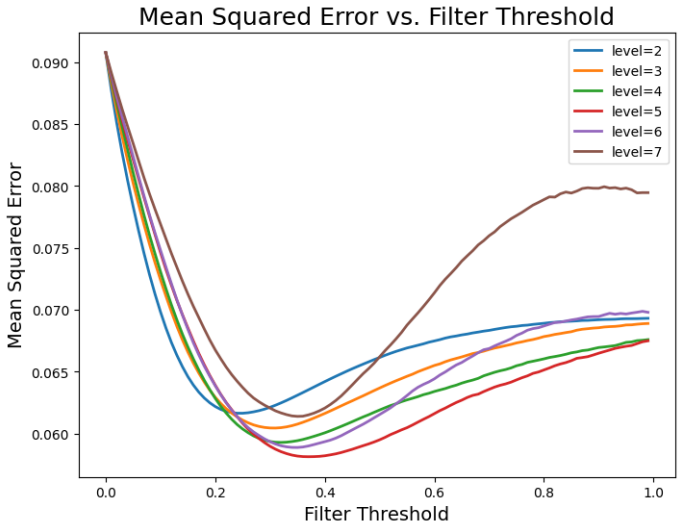

Figure 8: MSE as a function of wavelet filter threshold parameter. Each curve corresponds to a different maximum decomposition level for the WPT.

We observe that the optimal configuration for denoising is achieved at decomposition level of 5 with a threshold value of $\lambda = 5$, as this combination yields the lowest mean squared error between the denoised and true signal. Lower thresholds ($\lambda < 0.2$) did not provide sufficient noise removal, while higher thresholds ($\lambda > 0.6$) excessively filtered and removed important signal features, increasing the recorded error. In terms of the decomposition level, shallower levels lacked the resolution to isolate fine time-frequency structures, resulting in worse performance. Deeper levels, on the other hand, may have overfit the noise or distort signal components due to excessive splitting.

Applying the optimal threshold and level values, Figure 9 illustrates the results of applying the WPT filter to three gravitational wave samples with varying SNRs.

4 Conclusions

We observe that the WPT filter is particularly effective at isolating the merger event, which appears as a sharp, high-amplitude burst close to the event time ($t = 0$). This success is due to the WPT filter's ability the preserve large wavelet coefficients while suppressing smaller ones, well-suited for capturing the abrupt, localized, frequency changes characteristics of mergers. However, the filter struggles to retain the lower-amplitude inspiral phase that occurs before the event ($t < 0$). This phase produces smaller coefficients dispersed across scales, which are more likely to fall below the

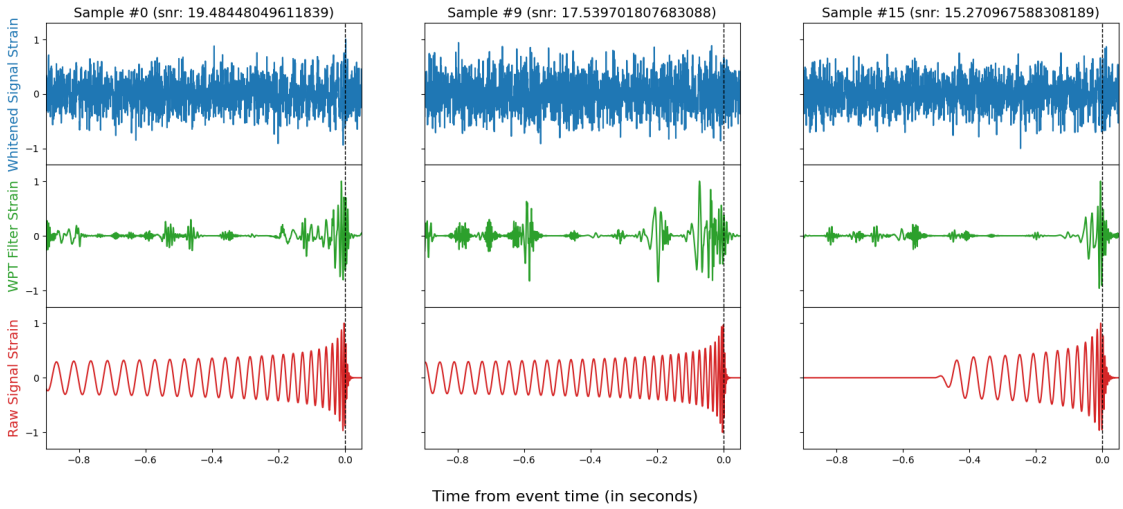

Figure 9: Denoised signals at different SNRs. Whitened signal on the top row (blue), WPT-denoised signal in the middle row (green), and true signal on the bottom row (red) for reference.

threshold and be attenuated or remove by the soft thresholding step. As a result, the inspiral signal is diminished or lost in the denoised output.

This trade-off highlights a limitation of threshold-based filtering in multiscale transforms. While they are effective at isolating dominant features like mergers, they may sacrifice subtle, distributed signal components like inspirals, critical for early detection and parameter estimation of the sources of CBC events. Unlike matched filtering methods, which incorporate physical waveform templates, this approach is entirely data-driven and non-parametric. While effective in enhancing the merger signal, the method struggles to fully retain the lower-amplitude inspiral phase due to aggressive coefficient thresholding and limited low-frequency resolution.

The data and code for this project is available at [2].

References

[1] Albert Boggess and Francis J. Narcowich. *A First Course in Wavelets with Fourier Analysis*. Wiley, 2nd edition, 2011.

[2] Macsen Casaus. wpt-cbc. `https://github.com/macsencasaus/wpt-cbc`, 2025.

[3] Timothy Gebhard and Niki Kilbertus. timothygebhard/ggwd: Version 1.0. `https://doi.org/10.5281/zenodo.2649359`, 2019.

[4] Timothy D. Gebhard, Niki Kilbertus, Ian Harry, and Bernhard Schölkopf. Convolutional neural networks: A magic bullet for gravitational-wave detection? *Physical Review D*, 100(6), September 2019.

[5] Gregory Lee, Roger Claypoole, Yanjun Fan, Tobias Kirchgessner, Nick Kovachki, Robert McGibbon, Hendrik Nahrstaedt, Jonas Reiss, Christof Schäfer, and Jose Unpingco. Pywavelets: A python package for wavelet analysis. *Journal of Open Source Software*, 4(36):1237, 2019.

[6] LIGO Scientific Collaboration. LIGO Algorithm Library—LALSuite. `https://doi.org/10.7935/GT1W-FZ16`, 2018. Free Software (GPL).

[7] LIGO Scientific Collaboration. LIGO Laboratory. `https://www.ligo.caltech.edu/`, 2024. Accessed: 2025-04-29.

[8] Mikhail Ryazanov. Wavelets-wpd. `https://en.wikipedia.org/wiki/File:Wavelets_-_WPD.png`, 2022. Accessed: 2025-04-29.

[9] Wikipedia Commons User:Johnteslade. Discrete wavelet transform. `https://commons.wikimedia.org/wiki/File:Wavelets_-_Filter_Bank.png`, 2005. Accessed: 2025-04-29.